Three-body recombination in two coupled Bose–Einstein condensates

2005 J. Phys. A: Math. Gen. 38 4105

(http://iopscience.iop.org/0305-4470/38/19/005)

INSTITUTE OF PHYSICS PUBLISHING JOURNAL OF PHYSICS A: MATHEMATICAL AND GENERAL

J. Phys. A: Math. Gen. **38** (2005) 4105–4114 doi:10.1088/0305-4470/38/19/005

Three-body recombination in two coupled Bose–Einstein condensates

Ya Li and Wenhua Hai

Department of Physics, Hunan Normal University, Changsha 410081, People's Republic of China

E-mail: whhai2005@yahoo.com.cn

Received 12 January 2005, in final form 30 March 2005
Published 25 April 2005
Online at stacks.iop.org/JPhysA/38/4105

Abstract

We investigate the dynamics of two Bose–Einstein condensates (BECs) tunnel coupled by a double-well potential. In the case of attractive interatomic interaction, the effects of the three-body recombination losses and the feeding of the condensates from the thermal cloud are studied by using a two-mode approximation. It is shown that the stability region of the parameter space could be enlarged by increasing the three-body losses or the tunnelling coefficient. The numerical results also reveal some interesting motion characteristics of the BECs for different s-wave scattering lengths, including macroscopic quantum self-trapping of non-stationary state BECs, and periodic oscillation of the population whose phase orbit tends to a stable limit cycle.

PACS numbers: 03.75.Lm, 32.80.Pj, 05.45.Ac, 05.30.Jp

1. Introduction

When Bose–Einstein condensation occurs in an atomic gas with attractive interaction [1–3], a metastable BEC is observed, where an upper critical number N_c of the ground state atoms exists [2]. Once the atomic number in the condensate exceeds the critical value, the atomic density becomes so high that the three-body recombination losses dominate over the attractive interaction, and the condensed atoms undergo a collapse that leads to a decrease of their number. As the number is reduced to a value that is less than N_c, the collapse is stopped and the condensate starts to grow, through feeding by the particle flux from the above-condensate cloud. Thus, the collapse and growth alternately occur such that the number of condensed atoms alternately varies. In the process of collapse and growth, three-body recombination plays an important role. The phenomenon of collapse and growth circulation has been verified by analysing the Gross–Pitaevskii equation (GPE) [2, 4, 5]. Numerical calculations performed by Filho *et al* show that the chaotic behaviour appears by changing the feeding parameter to enter the chaotic region [6]. By suddenly changing the atomic

interaction or the trapped potential, Muruganadan *et al* found that the BEC system tends to a long-term chaotic oscillation [7, 8]. The variation approach can also be used to estimate the stability region around the loss term and the feeding term [9]. The results in [2–7] are mainly based on numerical methods to study the collapse and growth of a single BEC in a harmonic potential. In this paper, however, we will combine analytical work with the numerical method to investigate the new effects of three-body recombination to a tunnel-coupled BEC pair [10] in a double-well potential. Very recently, the macroscopic quantum self-trapped phenomenon has been experimentally observed in a double well [11], which provides laboratory support for the theory for the two-mode approximation.

It is well known that inelastic collisions result in the loss of condensed atoms, including dipolar relaxation and three-body recombination. In this paper, we consider three-body recombination only and ignore dipolar relaxation. Three-body losses occur when three atoms scatter to form a molecular bound state and a third atom. The high kinetic energy of the final-state particles allows them to escape from the double-well potential [12]. It is of importance that three-body recombination only leads to the loss of atoms and does not break the coherence between the particles, which is retained by the trapped potential. Hence, the GPE must contain an imaginary three-body term to describe the recombination losses. By adjusting the value of the s-wave scatter length a, both the two-body interaction and the three-body recombination rates will be affected. Therefore, they cannot be controlled independently through the parameter a. However, given that the two-body interaction is proportional to a, while the three-body recombination rate grows as a^4 [12, 13], it is not hard to see that the relative change of the three-body recombination rates is larger than that of the two-body interaction for the same update of a. Consequently, for a fixed feeding term, the transition from the stationary state to the periodic oscillation state can be realized by decreasing a, as we show in this paper. The numerical plots of the phase orbits and time evolutions of the relative population show many interesting properties such as macroscopic quantum self-trapped and periodic motion with phase orbit being a limit cycle, which are associated with different values of the s-wave scattering length a by the Feshbach resonance.

This paper is organized as follows. After the introduction, we develop the two-mode approximation for the modified GPE including the imaginary interaction terms and derive three basic equations describing the BECs in a symmetric trap. Section 3 presents a stability analysis of the stationary solution, showing the dependence of stability on the three-body recombination and atomic feeding. In section 4, we study the motion characteristics of the BEC system by drawing the phase orbits numerically for the s-wave scattering lengths. Finally, we summarize and conclude our paper in section 5.

2. The two-mode approximation

The relation between the three-body recombination losses and the condensate density $n(\vec{r}, t) = |\Psi|^2$ has been described as [2] $\dot{n}(\vec{r}, t) = -\alpha_r n^3(\vec{r}, t)$, where $\alpha_r = C(\hbar/m)a^4$ is the recombination rate constant with m being the atomic mass and C being a constant, which can be adjusted in a large region [12, 13]. This could contribute an imaginary interaction term proportional to $|\Psi|^4\Psi$ into the GPE. Therefore, two tunnel-coupled BECs in a double-well potential with the recombination losses and the atomic feeding are governed by the modified GPE [2, 6, 7, 14],

$$\mathrm{i}\hbar\partial_t\Psi(\vec{r}, t) = \left[-\frac{\hbar^2}{2m}\nabla^2 + V_{\mathrm{ext}}(\vec{r}, t) - g|\Psi(\vec{r}, t)|^2 - \mathrm{i}\xi'|\Psi(\vec{r}, t)|^4 + \mathrm{i}\gamma\right]\Psi(\vec{r}, t). \tag{1}$$

We will study the attractive atoms ^{85}Rb, where a is negative and $g = 4\pi\hbar^2|a|/m$. The parameters $\xi' = \alpha_r\hbar/2$ and γ represent the strengths of the recombination losses in the condensates and the feeding by the particle flux from the nonequilibrium thermal cloud. They are two small positive constants in a practical situation. We consider the cigar-shaped potential $V_{\rm ext}(\vec{r}, t)$ with a harmonic confinement in the transverse dimensions and a double-well potential in the longitudinal dimension, which includes a harmonic term [14]. When the radial frequency ω_r is large enough, we can approximate the transverse wavefunction as the harmonic-oscillator ground state [15] such that equation (1) becomes the quasi-one-dimensional GPE [16].

$$\mathrm{i}\partial_\tau\tilde{\Psi}(x,\tau) = [-\nabla^2 + V_{\rm ext}(x,\tau) - A|\tilde{\Psi}(x,\tau)|^2 - \mathrm{i}\xi|\tilde{\Psi}(x,\tau)|^4 + \mathrm{i}\gamma]\tilde{\Psi}(x,\tau). \tag{2}$$

Here, the axial coordinate x is expressed in units of l_x and the dimensionless time $\tau = \omega_x t$, where l_x denotes the harmonic-oscillator length, $l_x = \sqrt{\hbar/(m\omega_x)}$, and ω_x is the harmonic frequency of the double well. The function $\tilde{\Psi} = \Psi/\tilde{n}^{1/2}$ is the normalized wavefunction and $\tilde{n} = (4|a_s|\omega_r/(l_x\omega_x))^{-1}$. The parameters ω_x, ω_r and $|a_s|$ are in order of 10^2 s^{-1}, 10^3 s^{-1} and 10^{-9} m, respectively. The new three-body parameter reads $\xi = CA^4|a_s|^2/\left(48\pi^2 l_x^2\right)$ and the constant $C = 1000$ will be used, as in Borca's work [13]. The dimensionless s-wave scattering length is rewritten as $A = a/a_s$ with a_s being a fixed parameter.

To investigate the dynamics of BECs in the double-well potential, we look for the solution of equation (2) in the form of the two-mode approximation [17–23],

$$\tilde{\Psi}(x,\tau) = \psi_1(\tau)\Phi_1(x) + \psi_2(\tau)\Phi_2(x). \tag{3}$$

Only when the two BECs are weakly coupled, the two-mode approximation could be a good approximation. The weak couple means that the spatial distribution functions $\Phi_1(x)$ and $\Phi_2(x)$ are localized in each well with a very weak overlap such that they satisfy the orthonormalization relation

$$\int \Phi_i^*(x)\Phi_j(x)\,\mathrm{d}x = \delta_{ij}, \qquad \text{for} \quad i, j = 1, 2. \tag{4}$$

This requires a higher barrier between the two wells and a smaller number of atoms in each well. Therefore, for a given double-well potential with the higher barrier the two-mode approximation can be safely used when the number of condensed atoms is less than the critical value N_c. In general, as a simple variational estimate, the spatial wavefunctions $\Phi_i(x)$ are assumed as a Gaussian profile $\Phi(x)$ that obeys $\Phi_i(x) = \Phi(x - x_i)$ with $x = x_i$ being the centre of the ith wavepacket [24] which is determined by $\mathrm{d}V_{\rm ext}/\mathrm{d}x = 0$. The width and normalization constant of the Gaussian waves $\Phi(x - x_i)$ depend on the value $\mathrm{d}^2V_{\rm ext}/\mathrm{d}x^2|_{x=x_i}$. Substituting equation (3) into equation (2) and using equation (4), after some integrations we obtain a pair of nonlinear equations

$$\mathrm{i}\partial_\tau\psi_1 = (E_1 - U_1|\psi_1|^2)\psi_1 - K\psi_2 + \mathrm{i}(\gamma - U_1'|\psi_1|^4)\psi_1, \tag{5}$$

$$\mathrm{i}\partial_\tau\psi_2 = (E_2 - U_2|\psi_2|^2)\psi_2 - K\psi_1 + \mathrm{i}(\gamma - U_2'|\psi_2|^4)\psi_2, \tag{6}$$

where E_i, U_i, K and U_i' for $i = 1, 2$ express the overlap integrations

$$E_i = \int [|\nabla\Phi_i|^2 + |\Phi_i|^2 V_{\rm ext}]\,\mathrm{d}x, \tag{7}$$

$$U_i = A\int |\Phi_i|^4\,\mathrm{d}x, \tag{8}$$

$$K = -\int [|\nabla\Phi_1\cdot\nabla\Phi_2| + \Phi_1 V_{\rm ext}\Phi_2]\,\mathrm{d}x, \tag{9}$$

$$U_i' = \xi\int |\Phi_i|^6\,\mathrm{d}x. \tag{10}$$

Therefore, these are some constants when the trapped potential $V_{\rm ext}$ depends only on the spatial coordinates. Given the double-well potential, we can construct the Gaussian waves $\Phi_i(x)$ and calculate the constants E_i, U_i, K and U_i'. Here, E_1 and E_2 represent the zero-point energies for each condensate; U_1 and U_2 are proportional to the mean-field interaction between atoms; K describes the tunnelling dynamics of the two condensates; and U_1' and U_2' are the three-body recombination interaction energies, which are proportional to ξ.

We set $\psi_i(\tau) = \sqrt{N_i(\tau)}\exp[\mathrm{i}\theta_i(\tau)]$ for $i = 1, 2$ so that the time dependence of the wavefunction $\tilde{\Psi}(x, \tau)$ is contained in $N_{1,2}$ and $\theta_{1,2}$, where $N_i(\tau)$ is the number of particles in the ith trap and is expressed in units of $(4a_s\omega_r/(l_x\omega_x))^{-1}$ and $\theta_i(\tau)$ is the phase of state ψ_i. The normalization condition reads $N_1 + N_2 = N$, where N is the total number of atoms of the two condensates with the same unit as N_i. We then make the function transformations [19]

$$\begin{aligned} u &= \psi_2^*\psi_1 + \psi_2\psi_1^*, \qquad & v &= -\mathrm{i}(\psi_2\psi_1^* - \psi_2^*\psi_1), \\ \eta &= \psi_2^*\psi_2 - \psi_1^*\psi_1, \qquad & N &= \psi_2^*\psi_2 + \psi_1^*\psi_1, \end{aligned} \tag{11}$$

where u and v characterize the coherence of the condensates, η is the relative population between two condensates and N is the time-dependent number of atoms, which satisfy $u^2 + v^2 + \eta^2 = N^2$. Inserting equation (11) into equations (5) and (6) yields the group of equations

$$\frac{\mathrm{d}u}{\mathrm{d}\tau} = v(\Delta E - \alpha N - \beta\eta) + u\left(2\gamma - \beta'\frac{N^2+\eta^2}{2} - \alpha' N\eta\right), \tag{12}$$

$$\frac{\mathrm{d}v}{\mathrm{d}\tau} = -2K\eta - u(\Delta E - \alpha N - \beta\eta) + v\left(2\gamma - \beta'\frac{N^2+\eta^2}{2} - \alpha' N\eta\right), \tag{13}$$

$$\frac{\mathrm{d}\eta}{\mathrm{d}\tau} = 2Kv + 2\gamma\eta - \alpha' N\frac{N^2+3\eta^2}{2} - \beta'\eta\frac{3N^2+\eta^2}{2}, \tag{14}$$

$$\frac{\mathrm{d}N}{\mathrm{d}\tau} = 2\gamma N - \alpha'\eta\frac{3N^2+\eta^2}{2} - \beta' N\frac{N^2+3\eta^2}{2}. \tag{15}$$

Here, we have defined the dimensionless parameters by $\Delta E = E_2 - E_1$, $\alpha = (U_2 - U_1)/2$, $\alpha' = (U_2' - U_1')/2$, $\beta = (U_2 + U_1)/2$ and $\beta' = (U_2' + U_1')/2$.

For simplicity, we only consider the case of symmetric potential. In this case, we have $U_1 = U_2 = U = \beta$, $U_1' = U_2' = U' = \beta'$, $\Delta E = E_2 - E_1 = 0$ and $\alpha = \alpha' = 0$. By introducing the relative phase $\phi = \theta_1 - \theta_2$, equations (12)–(15) can be rewritten as

$$\frac{\mathrm{d}N}{\mathrm{d}\tau} = 2\gamma N - U' N\frac{N^2+3\eta^2}{2}, \tag{16}$$

$$\frac{\mathrm{d}\eta}{\mathrm{d}\tau} = -2K\sqrt{N^2-\eta^2}\sin\phi + 2\gamma\eta - U'\eta\frac{3N^2+\eta^2}{2}, \tag{17}$$

$$\frac{\mathrm{d}\phi}{\mathrm{d}\tau} = -U\eta + 2K\frac{\eta}{\sqrt{N^2-\eta^2}}\cos\phi. \tag{18}$$

When γ and U' equate to zero, equations (16)–(18) are consistent with those obtained by Smerzi *et al* [17]. In their case, N is a constant. However, because of the three-body recombination losses and the atomic feeding from the above-condensate cloud, N is time-dependent in our case. Due to the two imaginary interaction terms, there are many new characteristics in the system. In the underlying sections, we will investigate some of the characteristics, through the adjustments of the three-body losses by changing the s-wave scattering length.

3. Stability analysis of the stationary solutions

In this section, we study the stability of the stationary solutions. When the left-hand sides of equations (16)–(18) are equal to zero, we can obtain multiple nonzero stationary solutions. Obviously, for $\eta = 0$, there are many groups of solutions: $N_0 = 2\sqrt{\gamma/U'}$, $\eta_0 = 0$ and $\phi_0 = k\pi$ for $k = 0, \pm1, \pm2, \ldots$. For $\eta \neq 0$, from equations (16)–(18) with $\dot{N} = 0, \dot{\eta} = 0, \dot{\phi} = 0$ we arrive at the equation of η,

$$U'^2\eta^6 + (U^2 - 2\gamma U')\eta^4 + \left(\gamma^2 - \frac{2U^2\gamma}{U'} + K^2\right)\eta^2 + \frac{U^2\gamma^2}{U'^2} - \frac{K^2\gamma}{U'} = 0. \tag{19}$$

We know that there are at most six real solutions for this equation. The nonzero constant η corresponds to a macroscopic quantum self-trapping of the stationary state [25, 26]. Once η is solved, we can compute N and ϕ as $N = (4\gamma/U' - 3\eta^2)^{1/2}$, $\phi = \arcsin[(U'\eta^3 - \gamma\eta)/(K\sqrt{\gamma/U' - \eta^2})]$, respectively. By setting the coefficient of η^4 equal to zero and $y = \eta^2$, we simplify equation (19) as

$$y^3 + py + q = 0, \tag{20}$$

where $p = (K^2 - 3\gamma^2)/U'^2$ and $q = (2\gamma^3 - K^2\gamma)/U'^3$. Hence, from the well-known Cardan formula we can solve the equation, yielding

$$\begin{aligned}
y_1 &= \sqrt[3]{-q/2 + \sqrt{(q/2)^2 + (p/3)^3}} + \sqrt[3]{-q/2 - \sqrt{(q/2)^2 + (p/3)^3}},\\
y_2 &= \sigma\sqrt[3]{-q/2 + \sqrt{(q/2)^2 + (p/3)^3}} + \sigma^2\sqrt[3]{-q/2 - \sqrt{(q/2)^2 + (p/3)^3}},\\
y_3 &= \sigma^2\sqrt[3]{-q/2 + \sqrt{(q/2)^2 + (p/3)^3}} + \sigma\sqrt[3]{-q/2 - \sqrt{(q/2)^2 + (p/3)^3}},
\end{aligned}$$

where $\sigma = -1/2 + \mathrm{i}\sqrt{3}/2$. The positive real solutions of y lead to the corresponding real solutions of η. Note that the parameters U, γ and U' are positive. By analysing the solutions of equation (20), we find that for $K^2 \geqslant 2\gamma^2$ there is at most one positive real solution

$$y = \frac{1}{U'}\sqrt[3]{(K^2\gamma - 2\gamma^3) + \sqrt{K^4\left(\frac{K^2}{27} - \frac{\gamma^2}{12}\right)}} + \frac{1}{U'}\sqrt[3]{(K^2\gamma - 2\gamma^3) - \sqrt{K^4\left(\frac{K^2}{27} - \frac{\gamma^2}{12}\right)}}. \tag{21}$$

So η has at most two nonzero real solutions, $\eta = \pm\sqrt{y}$.

For simplicity, we take the case $\eta = 0$ as an example, where the stationary solutions are either in phase ($\phi = 0$) or out phase ($\phi = \pi$). We shall mainly discuss the stability of the stationary solution $N_0 = 2\sqrt{\gamma/U'}$, $\eta_0 = 0, \phi_0 = 0$. Let N', η' and ϕ' be the perturbation corrections to the stationary solutions so that $N = N_0 + N'$, $\eta = \eta_0 + \eta'$, $\phi = \phi_0 + \phi'$. Inserting them into equations (16)–(18) produces linearized equations of the matrix form

$$\frac{\mathrm{d}}{\mathrm{d}\tau}\begin{pmatrix} N' \\ \eta' \\ \phi' \end{pmatrix} = \begin{pmatrix} -4\gamma & 0 & 0 \\ 0 & -4\gamma & -4K\sqrt{\frac{\gamma}{U'}} \\ 0 & -U + K\sqrt{\frac{U'}{\gamma}} & 0 \end{pmatrix}\begin{pmatrix} N' \\ \eta' \\ \phi' \end{pmatrix}, \tag{22}$$

whose solutions describe the Lyapunov stability of the system [27, 28]. The eigenvalues of the coefficient matrix are $\lambda_1 = -4\gamma$, $\lambda_{2,3} = -2\gamma \pm 2\sqrt{\gamma^2 - (K^2 - KU\sqrt{\gamma/U'})}$. Obviously, when $K^2 - KU\sqrt{\gamma/U'} > 0$, all the eigenvalues, λ_i for $i = 1, 2, 3$, are negative such that the stationary solution is asymptotically stable [29–31]. For $K^2 - KU\sqrt{\gamma/U'} < 0$, there is at least a positive eigenvalue, indicating the instability of the stationary solution. For

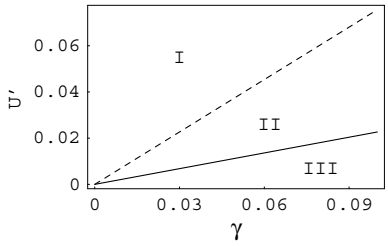

Figure 1. The stability region of the stationary solution in the (U', γ) plane. The critical lines are given from the equation $K^2 - KU\sqrt{\gamma/U'} = 0$ for $U = 1$, $K = 2.1$ (solid line) and $U = 1$, $K = 1.15$ (dashed line).

$K^2 - KU\sqrt{\gamma/U'} = 0$, one eigenvalue equates to zero and the others are negative. This is a critical situation for stability.

In figure 1, we plot the critical lines U' versus γ from $K^2 - KU\sqrt{\gamma/U'} = 0$ for $U = 1$, where the solid line is associated with $K = 2.1$ and the dashed line with $K = 1.15$, respectively. In this case, the stationary solution $N_0 = 2\sqrt{\gamma/U'}$, $\eta_0 = 0$, $\phi_0 = 0$ is stable so long as the parameters obey $U' > \gamma/K^2$. Thus, there are different stability regions corresponding to the different values of parameter K. When $K = 1.15$, the stationary solution is stable in region I, but is unstable in regions II and III. For $K = 2.1$, the region II above the solid critical line becomes the stability one, so the stability region is increased to I and II and the instability region is decreased to III. Therefore, the stability region of the system is enlarged as the increase of tunnelling parameter K. In the experiment, we can increase the tunnelling coefficient K by decreasing the height of the trapped potential so that the stability region can be modified in this way. This figure also shows that after increasing U' or decreasing γ the initially unstable system could enter the stable state for a fixed K value.

In the same way, we can obtain the stability region of the stationary solution in the (U, K) parameter plane. So we can also find that the stability region will diminish with decrease of the three-body losses. Thus, we can change the stability region by modifying the three-body loss term. In the experiment, the three-body loss parameter can be adjusted by using some mechanisms such as the Feshbach resonance for controlling the instability.

For the π-phase stationary solution $N_0 = 2\sqrt{\gamma/U'}$, $\eta = 0, \phi = \pi$, we can obtain the stability regions in the same way. We find the system is stable when the inequality $K^2 + KU\sqrt{\gamma/U'} > 0$ holds. The similar stationary state results will not be discussed here and the non-stationary features of the system will be illustrated numerically in the next section.

4. Numerical illustrations of the recombination effects

Using the two-mode approximation, we have obtained the time-dependent equations (16)–(18) when the trapped potential is symmetric. Although the equations seem to be simple, their analytic solutions [32] cannot been given due to the imaginary three-body loss and feeding terms. Therefore, in this section we shall use the software package 'Mathematica' [33] to perform numerical computations for illustrating the effects of the two imaginary interaction terms on the condensates in the symmetric double-well potential.

Firstly, we study the time evolutions of the relative population η. We know that the atoms ^{85}Rb with $a = -400a_0$ were considered in [29], where a_0 is the Bohr radius. In our paper, we take $a_s = -100a_0$ and adjust the s-wave scattering length $a = Aa_s$ by changing the value of A. Fixing the frequencies $\omega_x = 2\pi \times 16.3$ Hz and $\omega_r \approx 2\pi \times 160$ Hz, and employing the double-well potential $V_{\text{ext}}(x) = x^2 + b(\exp(-cx^2) - 1)$, where $b = 16$,

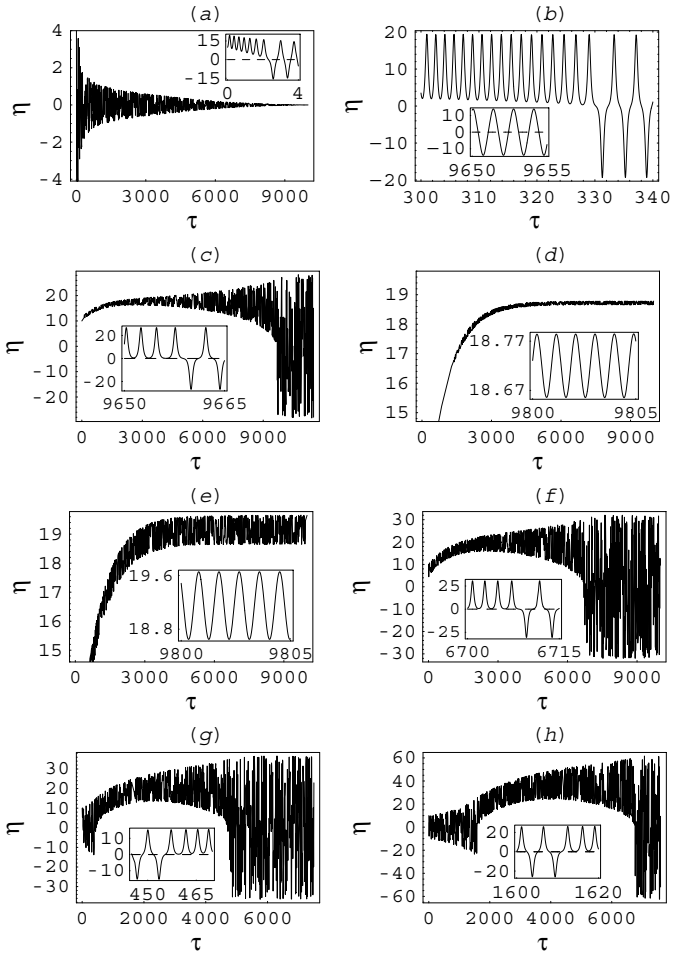

Figure 2. The time evolutions of the relative population η in units of $(4|a_s|\omega_r/(l_x\omega_x))^{-1}$ for the different values of the s-wave scattering length a. The initial conditions and physical parameters are set as $N(0) = 24, \eta(0) = 10, \phi(0) = 0, U = 0.7A, K = 3.9, \gamma = 1.6 \times 10^{-4}, U' = 0.05 \times 10^{-4}A^4$, and (*a*) $A = 2.61$; (*b*) $A = 0.7$; (*c*) $A = 0.52$; (*d*) $A = 0.511$; (*e*) $A = 0.506$; (*f*) $A = 0.49$; (*g*) $A = 0.46$; (*h*) $A = 0.35$.

$c = 18$ and x is normalized by l_x. From $\mathrm{d}V_{\mathrm{ext}}/\mathrm{d}x|_{x=x_i} = 0$ we get the distance $D = 2|x_i|$ of the double well, which is of micrometre order. This is in good agreement with recent experimental data [11]. Thus, we can calculate the constants E_i, U_i, K and U_i' from equations (7)–(10) and obtain the corresponding U and U'. Selecting the initial constants and physical parameters in the experimentally allowable regions as $N(0) = 24, \eta(0) = 10, \phi(0) = 0, U = 0.7A, K = 3.9, \gamma = 1.6 \times 10^{-4}, U' = 0.05 \times 10^{-4}A^4$ and gradually reducing A value, we plot the time evolutions of the relative population as shown in figure 2. In the numerical computation, we choose the maximum number of time steps as 2×10^6, and the step size is related to this number and the maximal evolution time. Here, the initial atomic number is about 312 particles. Note that the three-body parameter U' and 2-body one U are changed simultaneously with the change of A value. In figure 2(*a*) with $A = 2.61$, the initial atomic number is bigger than the stationary solution $N_0 = 2\sqrt{\gamma/U'}$ and the relative population η decays to zero after the dimensionless time $\tau = 9000$. The total number of particles and relative

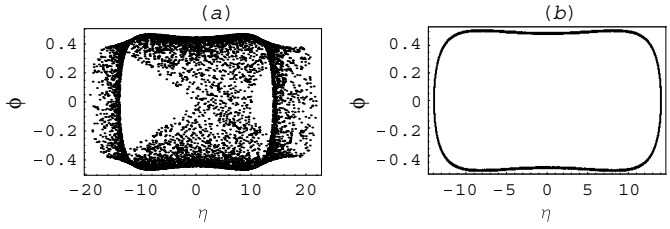

Figure 3. The limit cycles on the phase space ϕ versus η from equations (16)–(18) for (*a*) $U = 0.7A$, $K = 3.9$, $\gamma = 1.6 \times 10^{-4}$, $U' = 0.05 \times 10^{-4}A^4$, $A = 0.7$, $N(0) = 24$, $\eta(0) = 10$ and $\phi(0) = 0$; in (*b*) we show the orbit from $\tau = 8000$ to $\tau = 15\,000$, which tends to the limit cycle embedded in (*a*).

phase will reach the stationary state $N_0 = 2\sqrt{\gamma/U'}$ and $\phi_0 = k\pi$ for $k = 0, \pm1, \pm2, \ldots$ as η tends to zero. The nonzero average relative population implies the system being in the macroscopic quantum self-trapping state [25, 26]. And it can be observed before $\tau = 3$ or $t = 3\left(\omega_x^{-1}\right) \approx 29.3$ ms (see the inset). Moreover, we also find that the system will enter this stable stationary state for the above parameter set with $A > 2.6$. These are not exhibited in the figure. However, when $A < 2.6$, the system has many new properties as follows. In figure 2(*b*), with $A = 0.7$, we show that after some amplitude-decayed oscillations the relative population tends to a periodic oscillation (see the inset); however, unlike the previous case, the initial self-trapping will be kept for a longer time. A similar phenomenon can be observed for any $A \in (0.515, 2.6)$. In this A region, the smaller the value of A, the longer the time of the trapping state, and the amplitude of the relative population oscillation is larger. This can be seen in figures 2(*b*) and (*c*). When A continues decreasing to 0.511 in figure 2(*d*), the system is in a new quantum self-trapping state based on the periodic tunnelling. In the inset, we can see the amplitude of the relative population is very small. For $A \in [0.5058, 0.515]$, the system is self-trapping. And around $A = 0.511$, the amplitude is smaller than the others, as shown in figures 2(*d*) and (*e*). In this case, we can think that the self-trapping time is increasing to a large value. When A continues decreasing to 0.49 in figure 2(*f*), the time at which the trapping state exists is decreased. By further decreasing A to 0.487, a similar phenomenon, apart from the increase in the amplitude of η, can be kept in the process of further decreasing A. Moreover, in the above processes the time evolutions of ϕ also oscillate about $\phi_0 = 0$. Starting from $A = 0.486$, we find that although there is not the self-trapping state initially, it appears again after some time evolutions. In figure 2(*g*), the self-trapping state appears at about $\tau = 450$ and holds until $\tau = 4714$. By decreasing A, the time holding the amplitude-increased oscillations is increased as shown in figure 2(*h*). The larger amplitude is associated with the stronger tunnel effect in a period of motion. In this case, the total number of atoms will reach about 830. With a further decrease in the value of A, the amplitude of η, the time holding the beginning oscillation state and the self-trapping state will all be increased. Hence, we can adjust the three-body loss strength using the Feshbach resonances to control the motions to one of the periodic and stationary states. Note that some plots in figure 2 are dense and smooth, but are not to be confused, due to the long evolution time. In order to see them clearly, we present an inset in every figure.

It is worth noting that in most of the above-mentioned cases there exist the metastable macroscopic quantum self-trapping states for certain times, and the system enters either the stable periodical motion or the stationary state finally for any case, through macroscopic quantum tunnelling. These can also be illustrated by the orbits on the phase space as follows.

Now we present the orbits on the phase space of the phase difference ϕ versus the relative population η, where a limit cycle is shown. We take the same initial conditions and fixed parameters as those in figure 2(b). In this case, η is a periodic function of τ as time evolves. In figure 3(a), the initial point $(N(0) = 24, \eta(0) = 10, \phi(0) = 0)$ is taken inside of the limit cycle for $A = 0.7$. The phase orbits are plotted for the dimensionless time from 0 to 15 000. For the cases in figure 3(a) the system moves inside of the limit cycle and arrives at the cycle finally. At the beginning, it can overrun the limit cycle. If the outside point $(N(0) = 24, \eta(0) = 22, \phi(0) = 0)$ of the cycle for the same A value is taken initially, the plot is similar to figure 3(a). After some non-periodical oscillations, all of the orbits of above tend to the limit cycle in figure 3(b) at $\tau \approx 8000$ and hold on the cycle after this time. Therefore, the cycle in figure 3(b) is a limit cycle that indeed shows the stability and periodicity of the motions for the given conditions. More computations show that the relative phase will tend to instability such that the limit cycle may be destroyed with the decrease of the parameter A. In figure 3, we do not select a continuous curve to replace the real scattered points, since the auto-jointers between these scattered points will lead to the curve being a very dense one.

In the numerical computations, we have considered the requirement of the two-mode approximation to the weak tunnel-couple with the small atomic sample. We initially take the total number of particles to be about $N = (4|a_s|\omega_r/(l_x\omega_x))^{-1}N(0) \approx 12.98 \times 24 \approx 312$, where the parameter $N(0) = 24$ has been chosen. Because of the effect of the feeding from the thermal cloud on the condensates, the total number of atoms will reach about $N = 830$, as shown in figure 2. If we increase this number to $N = 10^4$ and fix the other parameters as those shown in figure 2(g), the tunnel-couple is no longer weak such that the relative population decays to zero in the two-mode approximation.

5. Conclusions and discussions

We have analysed the effects of three-body recombination losses on a condensates tunnel coupled by a double-well potential. Our approach is based on a simplified two-mode approximation. In this way, we investigated the modified GP equation and obtained three ordinary differential equations (16)–(18) in the case of the symmetric trapped potential. The stationary and non-stationary features of the system have been discussed analytically and numerically from these equations.

We first identified the stability regions of the stationary solutions and found that the stability region can be enlarged with the increase in the tunnelling coefficient K or the three-body loss strength U'. We then used the software package 'Mathematica' to numerically calculate the time evolutions of the relative population η. The numerical work has demonstrated many interesting characteristics of the system, which correspond to different values of the three-body loss parameter U' by changing the s-wave scattering length. The results showed that when the value of A is relatively lager as in figure 2(a), the system decays to the stable stationary state without macroscopic quantum self-trapping. Decreasing the value of A to that of figures 2(b)–(h) leads to the case where the relative population η becomes periodic with nonzero average values that implies macroscopic quantum self-trapping. The results reveal that we can control the transitions between the stationary states and periodic states with quantum self-trapping, by adjusting the s-wave scattering length of the system.

The two-mode theory, which is a simple model, has already provided some interesting properties of the system in the symmetric double-well potential. We hope that the homoclinic solution of equations (12)–(15) can be carried out and the Melnikov chaos can be found by using the perturbation method [34] and time-dependent asymmetric potential $V_{\rm ext}$ [18–22].

Furthermore, we can analyse the stationary chaotic behaviour and identify the corresponding chaotic region in the parameter space [35].

Acknowledgment

This work was supported by the National Natural Science Foundation of China under grant no 10275023.

References

[1] Dalfovo F, Giorgini S, Pitaevskii L P and Stringari S 1999 *Rev. Mod. Phys.* **71** 463
[2] Kagan Y, Muryshev A E and Shlyapnikov G V 1998 *Phys. Rev. Lett.* **81** 933
[3] Bradley C C, Sckett C A and Hulet R G 1997 *Phys. Rev. Lett.* **78** 985
[4] Berge L and Juul Rasmussen J 2002 *Phys. Lett.* A **304** 136
[5] Saito H and Ueda M 2001 *Phys. Rev. Lett.* **86** 1406
[6] Filho V S, Gammal A, Frederico T and Tomio L 2000 *Phys. Rev.* A **62** 033605
[7] Muruganandan P and Adhikari S K 2002 *Phys. Rev.* A **65** 043608
[8] Coullet P and Vandenberghe N 2002 *J. Phys. B: At. Mol. Opt. Phys.* **35** 1593
[9] Filho V S, Abdullaev F K, Gammal A and Tomio L 2001 *Phys. Rev.* A **63** 053603
[10] Zhou H-Q, Links J, McKenzie R H and Guan X-W 2003 *J. Phys. A: Math. Gen.* **36** L113
[11] Alblez M, Gati R, Fölling J, Hunsmann S, Cristiani M and Oberthaler M K 2004 Direct observation of tunneling and nonlinear self-trapping in a single bosonic Josephson junction *Preprint* cond-mat/0411757
[12] Braaten E and Hammer H W 2001 *Phys. Rev. Lett.* **87** 160407
[13] Esry B D, Greene H C and Burke J P Jr 1999 *Phys. Rev. Lett.* **83** 1751
Borca B, Dunn J W, Kokoouline V and Greene C H 2003 *Phys. Rev. Lett.* **91** 070404
Fedichev P O, Reynolds M W and Shlyapnikov G V 1996 *Phys. Rev. Lett.* **77** 2921
Bedaque P F, Braaten E and Hammer H W 2000 *Phys. Rev. Lett.* **85** 908
[14] Milburn G J, Corney J, Wright E M and Walls D F 1997 *Phys. Rev.* A **55** 4318
[15] Andrews M R, Townsend C G, Miesner H J, Durfee D S, Kurn D M and Ketterle W 1997 *Science* **275** 637
Thomas N R and Wilson A C 1999 *Phys. Rev.* A **65** 063406
Tiecke T G, Kemmann M, Buggle C, Shvarchuck I, Klitzing W V and Walraven J T M 2003 *J. Opt. B: Quantum Semiclass. Opt.* **5** S119
[16] Gardiner S A, Jaksch D, Dum R, Cirac J I and Zoller P 2000 *Phys. Rev.* A **62** 023612
Salasnich L, Parola A and Reatto L 2003 *Phys. Rev. Lett.* **91** 080405
Hai W, Lee C and Chong G 2004 *Phys. Rev.* A **70** 053621
[17] Smerzi A, Fantoni S, Giovanazzi S and Shenoy S R 1997 *Phys. Rev. Lett.* **79** 4950
[18] Hai W, Lee C, Chong G and Shi L 2002 *Phys. Rev.* E **66** 026202
[19] Lee C, Hai W, Shi L, Zhu X and Gao K 2001 *Phys. Rev.* A **64** 053604
[20] Lee C, Hai W, Luo X, Shi L and Gao K 2003 *Phys. Rev.* A **68** 053614
Lee C, Hai W, Shi L and Gao K 2004 *Phys. Rev.* A **69** 033611
[21] Chong G, Hai W and Xie Q 2004 *Chaos* **14** 217
[22] Xie Q, Hai W and Chong G 2003 *Chaos* **13** 801
[23] Coullet P and Vandenberghe N 2001 *Phys. Rev.* E **64** 025202
[24] Cataliotti F S, Burger S, Fort C, Maddaloni P, Minardi F, Trombettoni A, Smerzi A and Inguscio M 2001 *Science* **293** 843
[25] Raghavan S, Smerzi A, Fantoni S and Shenoy S R 1999 *Phys. Rev.* A **59** 620
[26] Kuang L M and Ouyang Z W 2000 *Phys. Rev.* A **62** 023610
[27] Liu B Z and Peng J H 2004 *Nonlinear Dynamics* (Beijing: Advanced Education Publishing House) (in Chinese)
[28] Gammal A, Frederico T, Tomio L and Chomaz Ph 2000 *Phys. Rev.* A **61** 051602
[29] Cornish S L, Claussen N R, Roberts J L, Cornell E A and Wieman C E 2000 *Phys. Rev. Lett.* **85** 1795
[30] Adhikari S K 2001 *Phys. Lett.* A **281** 265
Adhikari S K 2001 *J. Phys. B: At. Mol. Opt. Phys.* **34** 4231
[31] Gammal A, Frederico T, Tomio L and Abdullaev F Kh 2000 *Phys. Lett.* A **267** 305
[32] Hioe F T 1999 *J. Phys. A: Math. Gen.* **32** 2415
[33] Wolfram S 2000 *The Mathematica Book* (Champaign, IL: Wolfram Research, Inc.)
[34] Hai W, Duan Y and Zhu X *et al* 1998 *J. Phys. A: Math. Gen.* **31** 2991
[35] Chong G, Hai W and Xie Q 2004 *Phys. Rev.* E **70** 036213